

# A Comparison Between Broad Histogram and Multicanonical Methods

A. R. Lima,<sup>1</sup> P. M. C. de Oliveira,<sup>1</sup> and T. J. P. Penna<sup>1</sup>

*Received June 20, 1999; final January 5, 2000*

---

We discuss the conceptual differences between the broad histogram (BHM) and reweighting methods in general, and particularly the so-called multicanonical (MUCA) approaches. The main difference is that BHM is based on microcanonical, fixed-energy averages which depend only on the good statistics taken *inside* each energy level. The detailed distribution of visits among different energy levels, determined by the particular dynamic rule one adopts, is irrelevant. Contrary to MUCA, where the results are extracted from the dynamic rule itself, within BHM any microcanonical dynamics could be adopted. As a numerical test, we have used both BHM and MUCA in order to obtain the spectral energy degeneracy of the Ising model in  $4 \times 4 \times 4$  and  $32 \times 32$  lattices, for which exact results are known. We discuss why BHM gives more accurate results than MUCA, even using *the same* Markovian sequence of states. In addition, such an advantage increases for larger systems.

---

**KEY WORDS:** Monte Carlo methods; Ising model; computational physics.

## I. INTRODUCTION

Development of tools for optimization of computer simulations is a field of great interest and activity. Cluster updating algorithms,<sup>(1-3)</sup> probability reweighting procedures<sup>(4-6)</sup> and, more recently, methods<sup>(7-9)</sup> that obtain directly the spectral degeneracy  $g(E)$  are a few examples of very successful approaches (for reviews of these methods see, for instance refs. 10-12 and references therein). The multicanonical (MUCA) and Broad Histogram (BHM) methods belong to the former category. The Entropic Sampling

---

<sup>1</sup> Instituto de Física, Universidade Federal Fluminense, 24210-340 Niterói, RJ, Brazil; e-mail: arlima@if.uff.br.

Method (ESM)<sup>(8)</sup> was proven to be an equivalent formulation of MUCA.<sup>(13)</sup> From the knowledge of  $g(E)$ , these methods allow us to obtain any thermodynamical quantity of interest for the system under study, as the canonical average

$$\langle Q \rangle_T = \frac{\sum_E g(E) \langle Q(E) \rangle \exp(-E/T)}{\sum_E g(E) \exp(-E/T)} \quad (1)$$

of some macroscopic quantity  $Q$  (magnetization, density, correlations, etc.). Both sums run over all allowed energies (for continuous spectra, they must be replaced by integrals),  $T$  is the fixed temperature, and the Boltzmann constant was set to unity. The degeneracy function  $g(E)$  simply counts the number of states with energy  $E$  (which, must be interpreted as a density within a narrow window  $dE$ , for continuous spectra). Also,

$$\langle Q(E) \rangle = \frac{\sum_{S[E]} Q_S}{g(E)} \quad (2)$$

is the microcanonical, fixed- $E$  average of  $Q$ . The sum runs *uniformly* over all states  $S$  with energy  $E$  (or, again, within the small window  $dE$ , for continuous spectra). Note that neither  $g(E)$  nor  $\langle Q(E) \rangle$  depend on the particular environment the system is actually interacting with, for instance the canonical heat bath represented by the exponential Boltzmann factors in Eq. (1). Thus, these methods go far beyond the canonical ensemble: once  $g(E)$  and  $\langle Q(E) \rangle$  were already determined for a given system, one can study its behavior under different environments, or different ensembles, using the same  $g(E)$  and  $\langle Q(E) \rangle$ . Accordingly, as an additional advantage, only one computer run is enough to evaluate the quantities of interest in a large range of temperatures and other parameters.

MUCA was introduced in 1991 by Berg and Neuhaus.<sup>(7)</sup> The basic idea of the method is to sample microconfigurations performing a biased random walk (RW) in the configuration space leading to another unbiased random walk (i.e., uniform distribution) along the energy axis. Thus, the visiting probability for each energy level  $E$  is inversely proportional to  $g(E)$ . By tuning the acceptance probability of movements in order to get a uniform distribution of visits along the energy axis, one is able to get  $g(E)$  at the end. MUCA has been proven to be very useful and efficient to obtain results in many different problems, such as first order phase transitions, confinement/deconfinement phase transition in SU(3) gauge theory, relaxation paths,<sup>(14)</sup> conformal studied of peptides, helix-coil transition and

protein folding, evolutionary problems<sup>(15)</sup> and to study phase equilibrium in binary lipid bilayer<sup>(16)</sup> (for reviews of the method see ref. 17).

BHM was introduced three years ago by de Oliveira *et al.*<sup>(18)</sup> It is based on an exact relation between the spectral degeneracy,  $g(E)$ , and the microcanonical averages of some special macroscopic quantities. A remarkable feature of BHM is its generality, since these macroscopic quantities can be averaged by different procedures.<sup>(18–29)</sup> Because it is not restricted to a rule like a biased random walk, more adequate dynamics can be adopted for each different application. BHM has been applied to a variety of magnetic systems such as the 2D and 3D Ising Models (also with external fields, next nearest neighbor interactions), 2D and 3D XY and Heisenberg Models, Ising Spin Glass<sup>(18–29)</sup> with accurate results in a very efficient way. Theoretically, the method can be applied to any statistical system.<sup>(21)</sup> Another distinguishing feature of *BHM* is that its numerical results do not rely on the number of visits  $H(E)$  to each energy level, a quantity which is updated by one unit for each new visited state. On the contrary, BHM is based on microcanonical averages of macroscopic quantities. Each visited state contributes with a macroscopic upgrade for the measured quantities. Thus the numerical accuracy is much better than that obtained within all other methods, better yet for larger and larger systems, considering the same computer effort.

Besides the practical points described above, the most important feature of BHM is the following conceptual one. All reweighting methods<sup>(4–9)</sup> depend on the final distribution of visits  $H(E)$  along the energy axis. Histogram methods<sup>(4–6)</sup> adopt a canonical dynamics, getting  $H_{T_0}(E)$  for some fixed temperature  $T_0$ ; a new distribution  $H_T(E)$  is then analytically inferred for another (not simulated) temperature  $T$ . Following the same reasoning, one can also obtain  $g(E)$ .<sup>(5)</sup> Multicanonical approaches,<sup>(7–9)</sup> on the other hand tune appropriate dynamics in order to obtain a flat distribution  $H(E)$ . In both cases, the actually implemented transition probabilities from energy level  $E$  to another value  $E'$  are crucial. In other words, in both cases the results depend on the comparison of  $H(E)$  with the neighboring  $H(E')$ . All those reweighting methods are, thus, extremely sensitive to the particular dynamic rule adopted during the computer run, i.e., to the prescribed transition probabilities from  $E$  to  $E'$ .

BHM is not a reweighting method. It does not perform any reweighting on the distribution of visits  $H(E)$ . It needs only the knowledge of the microcanonical, fixed- $E$  averages of some particular macroscopic quantities. The possible transitions from the current energy  $E$  to other values are *exactly* taken into account within these quantities (see Section III), instead of performing a numerical measurement of the corresponding probabilities during the computer run. Thus, the only important role played by the

actually implemented dynamic rule is to provide a good statistics *within each energy level, separately*: the relative weight of  $H(E)$  as compared to  $H(E')$ , i.e., the relative visitation frequency for different energy levels, is completely irrelevant. One can even decide to sample more states inside a particularly important region of the energy axis (near the critical point, for instance),<sup>(23)</sup> instead of a flat distribution. In short, any dynamic rule can be adopted within BHM, the only constraint is to sample with uniform probability the various states belonging to the same energy level not the relative probabilities concerning different energies.

In this paper we have used the formulation of MUCA given by Lee<sup>(8)</sup> called Entropic Sampling, which, from now on, we call ESM. We present a comparison between ESM/MUCA and BHM, focusing on both accuracy and the use of CPU time. We choose to start our study with the same example used in the original ESM paper by Lee:<sup>(8)</sup> the  $4 \times 4 \times 4$  simple cubic Ising model, for which the exact energy spectrum is known.<sup>(30)</sup> Our results show that BHM gives more accurate results than ESM/MUCA with the same number of Monte Carlo steps. Despite the fact that one Monte Carlo step in BHM takes more CPU time, in measuring further macroscopic averages, the overall CPU time is smaller for the same accuracy, at least for this model. Also, BHM can be applied to larger lattices without the problems faced by ESM/MUCA, as we show in our simulations of the same model in a  $32 \times 32$  lattice.

This paper is structured as follows: in Section II and III we review the implementation of ESM/MUCA and BHM (including a detailed description of the distinct dynamics adopted in this work). In Section IV our numerical tests are presented and discussed. Conclusions are in Section V.

## II. THE MULTICANONICAL METHOD

The idea of the Multicanonical method is to obtain the spectral degeneracy of a given system using a biased RW in the configuration space.<sup>(7, 8)</sup> The transition probability between two states  $X_{\text{old}}$  and  $X_{\text{new}}$  is given by

$$\tau(X_{\text{old}}, X_{\text{new}}) = e^{-[S(E(X_{\text{new}})) - S(E(X_{\text{old}}))]} = \frac{g(E_{\text{old}})}{g(E_{\text{new}})} \quad (3)$$

where  $S(E(X)) = \ln g(E)$  is the entropy and  $E(X)$  is the energy of state  $X$ . The transitional probability (3) satisfies a detailed balance equation and

leads to a distribution of probabilities where a state is sampled with probability  $\propto 1/g(E)$ . The successive visitations along the energy axis follow a uniform distribution. However,  $g(E)$  is not known, *a priori*. In order to obtain  $g(E)$ , Lee<sup>(8)</sup> proposes the following algorithm:

*Step 1.* Start with  $S(E) = 0$  for all states;

*Step 2.* Perform a few unbiased RW steps in the configuration space and store  $T(E)$ , the number of tossed movements to each energy  $E$  (in this stage,  $T(E) = H(E)$  because all movements are accepted);

*Step 3.* Update  $S(E)$  according to

$$S(E) = \begin{cases} S(E) + \ln T(E), & \text{if } T(E) \neq 0 \\ S(E), & \text{otherwise} \end{cases} \quad (4)$$

*Step 4.* Perform a much longer MC run using the transitional probability given by Eq. (3), storing  $T(E)$ .

*Step 5.* Repeat 3 and 4. This is considered one iteration.

This implementation is known to be quite sensitive to the lengths of the MC runs in steps 2 and 4. In Section IV we study, in two examples, how the accuracy depends on the total number and size of each iteration.

### III. THE BROAD HISTOGRAM METHOD

BHM<sup>(18)</sup> enables us to directly calculate the energy spectrum  $g(E)$ , without any need for a particular choice of the dynamics to be used.<sup>(19)</sup> Many distinct dynamic rules could be used, and indeed some were already tested.<sup>(18–29)</sup>

Within BHM, the energy degeneracy is calculated through the following steps (alternatively, other quantities could replace  $E$ ):

*Step 1.* Choice of a reversible protocol of allowed movements in the state space. Reversible means simply that for each allowed movement  $X_{\text{old}} \rightarrow X_{\text{new}}$  the back movement  $X_{\text{new}} \rightarrow X_{\text{old}}$  is also allowed. It is important to note that these movements are virtual, since they are not actually performed. In this work we take the flips of one single spin as the protocol of movements;

*Step 2.* For a configuration  $X$ , to compute  $N(X, \Delta E)$ , the number of possible movements that change the energy  $E(X)$  by a given amount  $\Delta E$ . Therefore  $g(E) \langle N(E, \Delta E) \rangle$  is the total number of movements between

energy levels  $E$  and  $E + \Delta E$ , according to the definition (2) of microcanonical averages;

*Step 3.* Since the total number of possible movements from level  $E + \Delta E$  to level  $E$  is equal to the total number of possible movements from level  $E$  to level  $E + \Delta E$  (step 1, above), we can write down the equation<sup>(18)</sup>

$$g(E)\langle N(E, \Delta E) \rangle = g(E + \Delta E)\langle N(E + \Delta E, -\Delta E) \rangle \quad (5)$$

The relation above is exact for any statistical model and energy spectrum.<sup>(21)</sup> It can be rewritten as

$$\ln g(E + \Delta E) - \ln g(E) = \ln \frac{\langle N(E, \Delta E) \rangle}{\langle N(E + \Delta E, -\Delta E) \rangle} \quad (6)$$

This equation can be easily solved for all values of  $E$ , after  $\langle N(E, \Delta E) \rangle$  is obtained by any procedure, determining  $g(E)$  along the whole energy axis. In cases where  $\Delta E$  can assume more than one value, Eq. (5) becomes an overdetermined system of equations. However, the spectral degeneracy can be obtained without need of solving all equations simultaneously, since the spectral degeneracy is the same for all values of  $\Delta E$ .

The exact Broad Histogram relation (5) is independent of the procedure by which  $\langle N(E, \Delta E) \rangle$  is obtained.<sup>(19–24)</sup> Therefore, virtually any procedure can be adopted in this task, for instance, an unbiased energy RW,<sup>(18)</sup> a microcanonical simulation,<sup>(22)</sup> or a mixture of both.<sup>(21, 23)</sup> Even the juxtaposition of histograms obtained through canonical simulations at different temperatures, a completely unphysical procedure, could be used, as in some of the results presented in ref. 19, and explicitly used in ref. 27 where BHM is reformulated under a transition matrix<sup>(31)</sup> approach. Here, we are going to introduce an alternative procedure, referred as Entropic Sampling-based Dynamics for BHM (ESDYN, hereafter). First, one implements ESM, as described in Section II, in order to perform the visitation in the configuration space. Additionally, for each visited state  $X$ , we store the values of  $N(X, \Delta E)$  cumulatively into  $E$ -histograms. Therefore, at the end we have two choices for the determination of the spectral degeneracy, either by using the entropy accumulated through  $T(E)$  (that is the traditional ESM/MUCA) or by using the accumulated  $\langle N(E, \Delta E) \rangle$  and the BHM relation, Eq. (5). Because of this special implementation, we can guarantee that exactly the same states are visited for both methods. Hence, the eventual difference in the performances reported in this work must be credited to the methods themselves and not to purely statistical factors.

The dynamic rule originally used in order to test BHM<sup>(18)</sup> prescribes an acceptance probability  $p = \langle N(E + \Delta E, -\Delta E) \rangle / \langle N(E, \Delta E) \rangle$ . Both the

numerator and the denominator are read from the currently accumulated histograms, and thus  $p$  varies during the simulation. Wang<sup>(24)</sup> has proposed a new approach: instead of using the dynamically updated values of  $\langle N(E, \Delta E) \rangle$  as in ref. 18, the transitional probabilities follow a previously obtained (from a canonical simulation, for example) distribution  $\langle N_{\text{fixed}}(E, \Delta E) \rangle$ , kept fixed during the simulation. An alternative and simpler derivation of Wang's dynamics can be done by using the BHM relation (5) itself. From this, we readily obtain that Wang's dynamics is the same as using the transitional probability  $p = g_{\text{fixed}}(E)/g_{\text{fixed}}(E + \Delta E)$  with approximated values  $g_{\text{fixed}}(E)$  kept fixed during the simulation. We refer to this dynamics as approximated Wang's dynamics, since  $\langle N_{\text{fixed}}(E, \Delta E) \rangle$  (or  $g_{\text{fixed}}(E)$ ) is actually only an approximation of the real  $\langle N(E, \Delta E) \rangle$  (or  $g(E)$ ). We will use the results obtained by ESM or BHM with ESDYN as inputs to the approximate Wang's dynamics. These dynamics will be called AWANG1 and AWANG2, respectively.

For comparison, we also implemented a dynamics that uses the ESM probabilities taken from the exact values of  $g(E)$ . It is worth noticing that, as pointed out in the previous paragraph, this is equivalent to Wang's proposal with exact values for  $\langle N_{\text{fixed}}(E, \Delta E) \rangle$ . We refer to this dynamics as WANG. Its purpose is only to test the accuracies of the other approaches, once one does not know the exact  $g(E)$  a priori, in real implementations.

#### IV. NUMERICAL TESTS

We start our comparison with the smallest system, since it is also present in the ESM original paper by Lee.<sup>(8)</sup> The partition function for the  $4 \times 4 \times 4$  simple cubic Ising model is exactly known.<sup>(30)</sup> It is given by the polynomial function.

$$Z(\beta) = \sum_{n=0}^{96} C(n) u^n \quad (7)$$

where  $u = \exp(-4\beta)$ ,  $\beta = 1/T$ ,  $T$  is the temperature. The energy spectrum is written in terms of the coefficients  $C(n)$  as  $g(E) = g(2n) = C(n)$  for  $n = 0$  to  $n = 96$ . For this model, only the first 49 coefficients are necessary by symmetry. The other 48 coefficients are mirror images of the first ones. Our results will be expressed in terms of  $S(E) = \ln g(E)$ .

In order to compare the entropies as obtained by both ESM and BHM, we normalize the entropy such that  $g(96) = 1$ , i.e.,  $S(96) = 0$ . This point corresponds to the center of the energy spectrum, or, alternatively, to infinite temperature. Of course, the error relative to the exact value

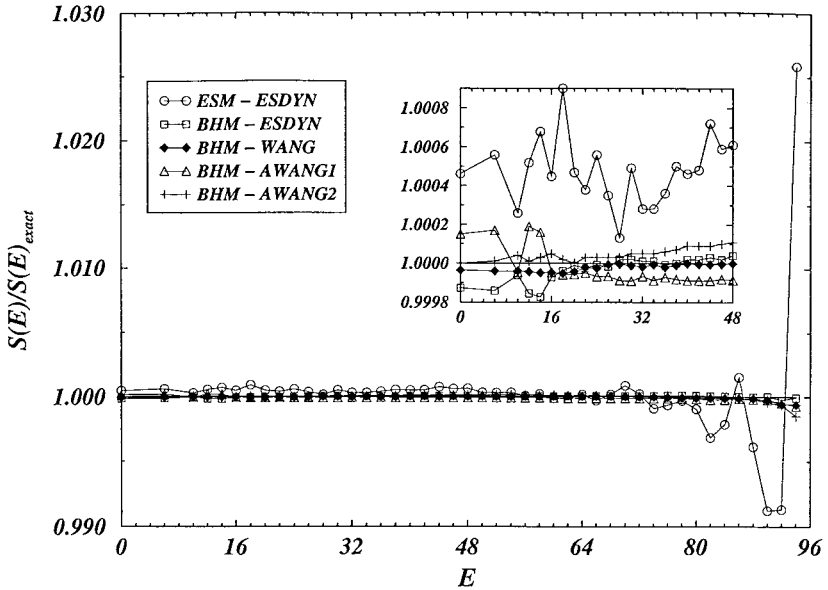


Fig. 1. Entropies (normalized by its exact values) for the  $4 \times 4 \times 4$  Ising ferromagnet, obtained by ESM/MUCA and BHM for 100 iterations of  $10^6$  Monte Carlo steps, each. The inset shows a detailed view of the first fourth of the whole spectrum. ESM/MUCA gives the largest errors. AWANG1 and AWANG2 dynamics also give worse results than BHM with both ES or WANG dynamics.

vanishes for  $E = 96$ . In Fig. 1, we compare the normalized (with respect to its exact value) entropy as function of  $E$  obtained by ESM and BHM (with four different dynamics). In AWANG1 and AWANG2 dynamics we use as  $\langle N_{\text{fixed}}(E, \Delta E) \rangle$  the results obtained by ESM and BHM with ESDYN, respectively. BHM with the entropic sampling dynamics or using the exact relation proposed by Wang present errors within the same order of magnitude, while pure ESM gives the worst results, as clearly seen in the inset. It is also clear the AWANG1 and AWANG2 results are worse than BHM with ESDYN.

The methods can be better compared by the ratio of their relative errors rather than their absolute values. We define the relative errors in the entropy, for a given energy  $E$ , as

$$\varepsilon(E) = \left| \frac{S(E) - S(E)_{\text{exact}}}{S(E)_{\text{exact}}} \right| \quad (8)$$



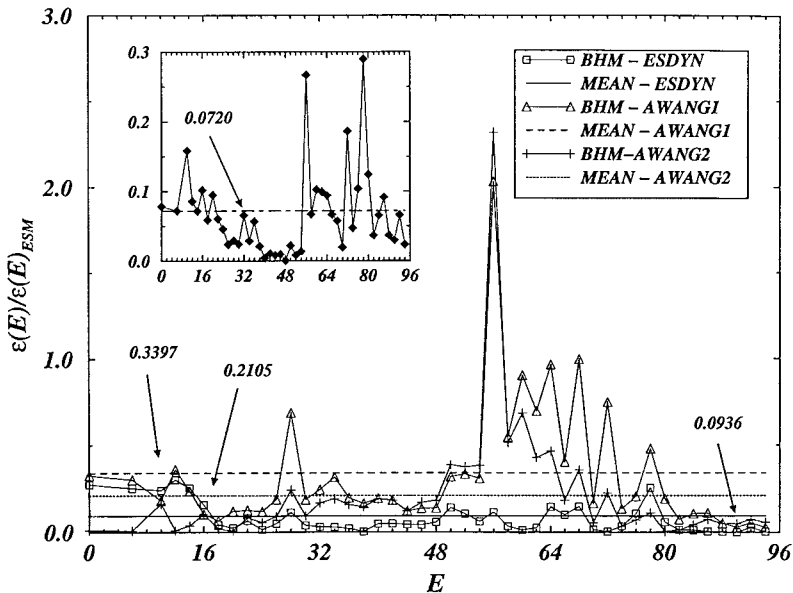


Fig. 2. Ratio between the relative errors for BHM and the ESM/MUCA ones. The horizontal lines are the mean relative errors. BHM is on average more than ten times more accurate than ESM/MUCA, for this number of iterations. The exact Wang's dynamics is, as expected, slightly more accurate than ESDYN (as shown in the inset) once it uses the exact  $g(E)$  as input in order to get  $g(E)$  as output. AWANG1 and AWANG2 give the worst results among the four distinct dynamics presently used in order to test BHM (see text).

In Fig. 2 we show the ratio between the BHM relative errors (obtained by ESDYN, AWANG1 and AWANG2 dynamics) and the ESM ones. The inset shows the ratio between the errors from BHM with WANG and the ESM ones. In its worst performance, the error obtained by BHM with ESDYN is roughly one third of the one obtained by ESM. BHM with Wang's exact dynamics gives slightly better results once it uses the exact  $g(E)$  as input in order to get  $g(E)$  as output. BHM with ESDYN gives on average results 11 times more accurate than ESM, for this number of iterations. However, BHM with the AWANG1 and AWANG2 dynamics give relatively poorer results. Therefore, we have shown that the ES dynamics is a powerful approach (among other possibilities<sup>(18-27)</sup>) to obtain with great accuracy the microcanonical averages  $\langle N(E, \Delta E) \rangle$  needed by BHM. Let us stress that the results for  $g(E)$  obtained with AWANG2 are worse than the input they use, namely the values of  $g(E)$  obtained as output of BHM with ESDYN. In order to obtain good results with Wang's dynamics, we need a pretty good estimative of  $g(E)$  as input, and not only some crude estimation as claimed in ref. 24.

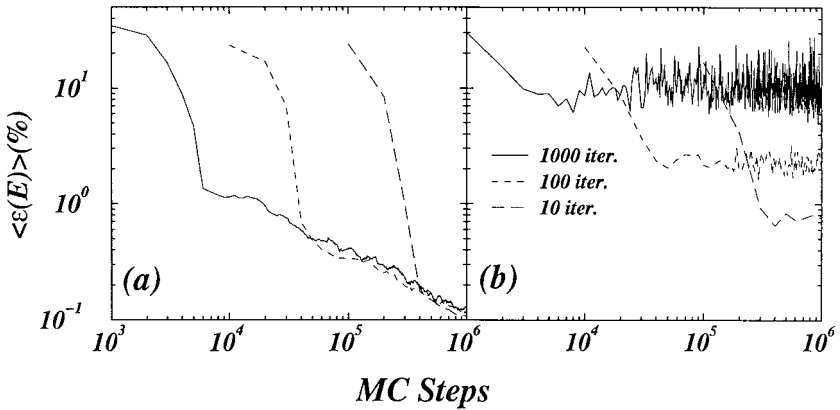


Fig. 3. Time evolution of the mean error for BHM with ESDYN (a) and ESM/MUCA (b). In both cases, exactly the same averaging states are visited: thus, the differences are due to the methods themselves, not to statistics. As described in the next, the entropic sampling dynamics is quite sensitive to the number of Monte Carlo steps between each iteration, that correspond to an update of the entropy. Here, we present the results for  $N = 10, 100, 1000$  iterations, that means  $10^5, 10^4$  and  $10^3$  Monte Carlo steps, respectively, between each iteration. The more Monte Carlo steps, the smaller is the error for the entropic sampling. Conversely BHM does not seem to depend on the computational strategy adopted. Moreover, the errors seem to stabilize after some steps, in the ESM case. On the contrary, for BHM, to get a better accuracy is a simple matter of increasing the computer time, once the errors decay as  $t^{-1/2}$ . The results are averaged over ten realizations.

In Fig. 3, we show the time evolution of the mean error as a function of the number of Monte Carlo steps (MCS). One iteration in ESM corresponds to perform many RW steps, according to Eq. (3), storing the number of visits at each energy and, after this fixed number of RW steps, to update the entropy, according to Eq. (4). As we pointed out before, the ESM performance is quite sensitive to the choice of the number of RW steps before each entropy update. For a fixed number of MCS ( $10^6$ ), we plot the time evolution for both ESM and BHM, but with different number of iterations. As one can see in Fig. 3, the best results for ESM correspond to the smaller number of iterations since, in this case, more RW steps are performed and, consequently, we have better statistics for the determination of the entropy.

It is worth noticing that the ESM/MUCA errors seem to stabilize after a few iterations. We believe that this effect occurs because the number of visits to each energy is not sufficient to provide a good statistics in determining the entropy. The only way to improve the accuracy in the spectral degeneracy is to perform more RW steps between each entropy update (it

does not increase the CPU time if the total number of MCS is kept constant). Conversely, for BHM the error decreases monotonically because macroscopic quantities are stored, leading to a good statistics even if some states are not frequently visited. After the very first steps, the errors decay as  $t^{-1/2}$ , as expected. It is also remarkable the accuracy when using BHM: we reach the same accuracy of the best performance of ESM/MUCA, by performing roughly 30 times less MCS.

Of course, accuracy is not the only important factor concerning the efficiency of a computational method. BHM with ES dynamics has one additional step compared to the traditional implementation of ESM, namely the storage of the macroscopic quantities  $N(X, \Delta E)$ . So, we need to know the cost of this additional step. In Table I, we show the CPU time (in seconds) spent in both implementations on a 433 MHz DEC Alpha, in order to obtain the results shown in Fig. 1. For direct comparison, we also present the CPU time relative to the ESM CPU time. All dynamics tested within BHM takes roughly the same CPU time. As one can see, BHM uses twice more CPU time than ESM. However, for the same number of steps, and the best strategy for ESM, BHM is at least 10 times more accurate. If we consider accuracy and CPU use, we argue that BHM is more efficient than ESM.

Up to now, we have tested both approaches in a very small lattice. Nevertheless, we can show that BHM is even more efficient for larger systems, as expected due to the macroscopic character of the quantities  $N(X, \Delta E)$ . For  $L^d$  Ising spins on a lattice, for instance, even restricting the allowed movements only to single-spin flips, the total number of movements

**Table I. CPU Time for Each Method and Dynamics<sup>a</sup>**

Method	Dynamics	CPU		
		Time(s)	$\frac{t}{t_{\text{ESM}}}$	$\frac{1}{\langle \varepsilon(E)/\varepsilon(E_{\text{ESM}}) \rangle}$
ESM	ESDYN	4181	1	1
BHM	AWANG1	9360	2.24	2.94
	AWANG2	9772	2.33	4.75
	ESDYN	8754	2.09	10.68

<sup>a</sup> ESM/MUCA is at least twice faster than BHM with the various dynamics used in this work. However, BHM is more than 10 times more accurate than the multicanonical approach. For AWANG1 dynamics, one must add the previous ESM time spent in determining  $\langle N_{\text{fixed}}(E, \Delta E) \rangle$ , i.e., 13541s. Analogously, AWANG2 spent a total time of 18526s. The simulations were carried out on a 433MHz DEC Alpha.

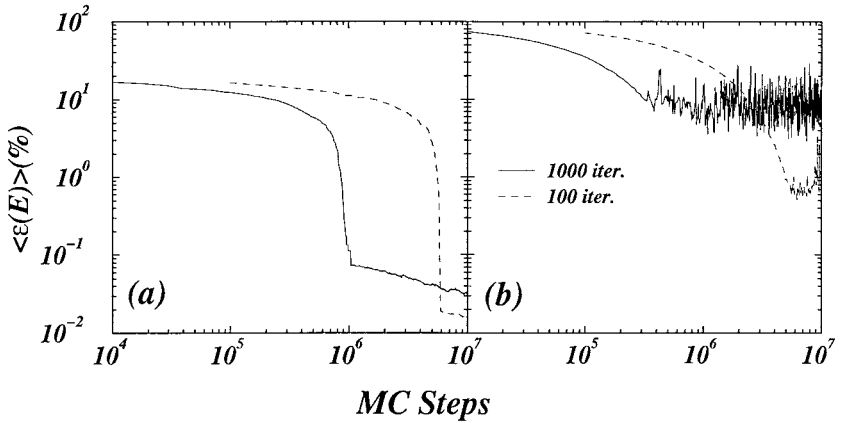


Fig. 4. Time evolution of the mean error for BHM with ESDYN (a) and ESM/MUCA (b) for the  $32 \times 32$  square lattice Ising Model. Now we consider  $10^7$  MC steps. Again we present the result for  $N=100$ , 1000 iterations, that means  $10^5$  and  $10^4$  Monte Carlo steps, respectively, between each iteration. The results are averaged over ten realizations. The ratio between the accuracies of BHM and ESM/MUCA is even higher for large systems.

starting from  $X$  is just  $L^d$ . Thus, being a finite fraction of them,  $N(X, \Delta E)$  is a macroscopic quantity (this is true along the whole energy axis, except at the ground state where  $g(E)$  presents a macroscopic jump relative to the neighboring energy levels). In Fig. 4 we present results for the time evolution of the mean error for a  $32 \times 32$  square lattice Ising model (a lattice that is 16 times larger than the one in the previous results). The exact solution for this system is also known.<sup>(32)</sup> Here, the accuracy of BHM is two orders of magnitude higher than that of ESM. Again the errors decrease as  $t^{-1/2}$  for BHM with ESDYN, while the ESM mean errors seem to stabilize. In summary, BHM with ESDYN can obtain accurate results for lattices much larger than the ones considered as limit for ESM.

## V. CONCLUSIONS

The Multicanonical<sup>(7,8)</sup> and the Broad Histogram<sup>(18)</sup> methods are completely distinct from canonical Monte Carlo methods, once they focus on the determination of the energy spectrum degeneracy  $g(E)$ . This quantity is independent of thermodynamic concepts and depends only on the particular system under study. It does not depend on the interactions of the system with the environment. Thus, once one has determined  $g(E)$ , the effects of different environments can be studied using always the same data for  $g(E)$ . Different temperatures, for instance, can be studied without need of a new computer run for each  $T$ .

The goal of this paper is to discuss the conceptual differences between Multicanonical and Broad Histogram frameworks, and to compare both methods concerning accuracy and speed. We obtained the energy spectrum of the Ising model in  $4 \times 4 \times 4$  and  $32 \times 32$  lattices, for which the exact results are known and, therefore, provide a good basis for comparison. Our findings show that a combination of the Broad Histogram method and the Entropic Sampling random walk dynamics (BHM with ESDYN) gives very accurate results and, in addition, it needs much less Monte Carlo steps to obtain the same accuracy as the pure Entropic Sampling method. This advantage of the Broad Histogram method grows with the system size, and it does not present the limitations of the Multicanonical or Entropic Sampling methods concerning large systems.

The reason for the better performance is that the BHM<sup>(18–29)</sup> uses the microcanonical averages  $\langle N(E, \Delta E) \rangle$ <sup>(18)</sup> of the macroscopic quantity  $N(X, \Delta E)$ —the number of potential movements which could be done starting from the current state  $X$ , leading to an energy variation of  $\Delta E$ . In this way, each new visited state contributes with a macroscopic value for the averages one measures during the computer simulation. Being macroscopic quantities, the larger the system, the more accurate are the results for these averages. Conversely, Histogram<sup>(4–6)</sup> and Multicanonical<sup>(7–9)</sup> approaches rely exclusively on  $H(E)$ , the number of visits to each energy. Therefore, each new averaging state contributes with only one more count to the averages being measured, i.e.,  $H(E) \rightarrow H(E) + 1$ , independent of the system size.

Under a conceptual point of view, BHM is also completely distinct from the other methods which are based on the final distribution of visits  $H(E)$ . Alternatively, it is based on the determination of microcanonical, fixed- $E$  averages  $\langle N(E, \Delta E) \rangle$ ,<sup>(18)</sup> concerning each energy level separately. Thus, the relative frequency of visitation between distinct energy levels, which is sensitive to the particular dynamic rule one adopts, i.e. the comparison between  $H(E)$  and  $H(E')$ , does not matter. The only requirement for the dynamics is to provide a uniform sampling probability for the states belonging to the same energy level. The transition probabilities from one level to the others are irrelevant.

## ACKNOWLEDGMENTS

This work has been partially supported by Brazilian agencies CAPES, CNPq and FAPERJ. The authors acknowledge D. C. Marcucci and J. S. Sá Martins for suggestions, discussions and critical readings of the manuscript.

## REFERENCES

1. A. Coniglio and W. Klein, *J. Phys. A* **13**:2775 (1980).
2. R. H. Swendsen, J.-S. Wang, and A. M. Ferrenberg, in *The Monte Carlo Method in Condensed Matter Physics*, K. Binder, ed. (Springer, Berlin), Topics in Applied Physics, Vol. 71, p. 75 (1992), and references therein.
3. U. Wolff, *Phys. Rev. Lett.* **62**:261 (1989).
4. Z. W. Salzburg, J. D. Jacobson, W. Fickett, and W. W. Wood, *J. Chem. Phys.* **30**:65 (1959).
5. R. Dickman and W. C. Schieve, *J. de Physique* **45**:1727 (1984).
6. R. W. Swendsen, *Physica A* **194**:53 (1993), and references therein.
7. B. A. Berg and T. Neuhaus, *Phys. Lett. B* **267**:249 (1991); B. A. Berg, *Int. J. Mod. Phys. C* **3**:1083 (1992).
8. J. Lee, *Phys. Rev. Lett.* **71**:211 (1993).
9. B. Hesselbo and R. B. Stinchcombe, *Phys. Rev. Lett.* **74**:2151 (1995).
10. E. Marinari, *Optimized Monte Carlo Methods*. Lectures given at the 1996 Budapest Summer School of Monte Carlo Methods, J. Kertész and I. Kondor, eds. (Springer, Berlin/Heidelberg, 1998), p. 50. Available at cond-mat/9612010.
11. J. R. D. de Felício and V. L. Libero, *Am. J. Phys.* **64**:1281 (1996).
12. M. E. J. Newman and G. T. Barkema, *Monte Carlo Methods in Statistical Physics* (Oxford, New York, 1999).
13. B. A. Berg, U. H. E. Hansmann, and Y. Okamoto, *J. Phys. Chem.* **99**:2236 (1995).
14. I. Shteto, J. Linares, and F. Varret, *Phys. Rev. E* **56**:5128 (1997).
15. M. Y. Cho, H. Y. Lee, and S. H. Parks, *J. Phys. A* **30**: L748 (1997).
16. G. Besold, J. Risbo, and O. G. Mouritsen, *Comput. Mat. Science* **15**:311 (1999).
17. B. A. Berg, in *Proceedings of the International Conference on Multiscale Phenomena and their Simulations*, F. Karsch, B. Monien, and H. Satz, eds. (Bielefeld, October 1996); (World Scientific, Singapore, 1997); W. Janke, *Physica A* **254**:164 (1988); B. Dünweg, in *Monte Carlo and Molecular Dynamics of Condensed Matter Physics*, K. Binder and C. Ciccotti, eds. (Como, July 1995); Società Italiana di Fisica, Bologna (1996), p. 215; B. A. Berg, U. H. E. Hansman, and T. Heuhaus, *Phys. Rev. B* **47**:497 (1993).
18. P. M. C. de Oliveira, T. J. P. Penna, and H. J. Herrmann, *Braz. J. Phys.* **26**:677 (1996). Available at cond-mat/9610041.
19. P. M. C. de Oliveira, T. J. P. Penna, and H. J. Herrmann, *Eur. Phys. J. B* **1**:205 (1998).
20. P. M. C. de Oliveira, in *Computer Simulation Studies in Condensed-Matter Physics XI*, D. P. Landau, ed. (Springer, Berlin, 1998), p. 196.
21. P. M. C. de Oliveira, *Eur. Phys. J. B* **6**:111 (1998). Available at cond-mat/9807354.
22. P. M. C. de Oliveira, *Int. J. Mod. Phys. C* **9**:497 (1998).
23. P. M. C. de Oliveira, CCP 1998 conference proceedings; *Comp. Phys. Comm.* **121–122**:16 (1999).
24. J.-S. Wang, *Eur. Phys. J. B* **8**:287–291 (1999); “Monte Carlo algorithms based on the number of potential moves” in cond-mat/990324.
25. J. D. Munoz and H. J. Herrmann, *Int. J. Mod. Phys. C* **10**:95 (1999); CCP 1998 conference proceedings, *Comp. Phys. Commun.*, also in *Computer Simulation Studies in Condensed-Matter Physics XII*, D. P. Landau, ed. (Springer, Berlin, in print) and cond-mat/981092.
26. A. R. Lima, J. S. Sá Martins, and T. J. P. Penna, *Physica A* **268**:553 (1999).
27. J. S. Wang, T. K. Tay, and R. H. Swendsen, *Phys. Rev. Lett.* **82**:476 (1999).
28. M. Kastner, J. D. Munoz, and M. Promberger, “Broad Histogram Method: Extension and Efficiency Test” in cond-mat/9906097.

29. A. R. Lima, P. M. C. de Oliveira, and T. J. P. Penna, *Solid State Comm.* **114**:447 (2000). Available at cond-mat/9912152.
30. R. B. Pearson, *Phys. Rev. B* **26**:6285 (1982).
31. G. R. Smith and A. D. Bruce, *J. Phys. A* **28**:6623 (1995); *Phys. Rev. E* **53**:6530 (1996); *Europhysics Lett.* **39**:91 (1996).
32. P. D. Beale, *Phys. Rev. Lett.* **76**:78 (1996).